

Experimental preparation of eight-partite linear and two-diamond shape cluster states for photonic qumodes

Xiaolong Su, Yaping Zhao, Shuhong Hao, Xiaojun Jia, Changde Xie, and Kunchi Peng*
*State Key Laboratory of Quantum Optics and Quantum Optics Devices,
 Institute of Opto-Electronics, Shanxi University, Taiyuan, 030006, People's Republic of China*

The preparation of multipartite entangled states is the prerequisite for exploring quantum information networks and quantum computation. In this letter, we present the first experimental demonstration of eight-partite spatially separated CV entangled states. The initial resource quantum states are eight squeezed states of light, through the linearly optical transformation of which two types of the eight-partite cluster entangled states are prepared, respectively. The generated eight entangled photonic qumodes are spatially separated, which provide valuable quantum resources to implement more complicated quantum information task.

PACS numbers: 03.67.Bg, 03.67.Lx, 03.65.Ud, 42.50.Dv

Developing quantum information (QI) science have exhibited unusual potentiality [1, 2]. Optical QI based on exploiting discrete-variable (DV) of single-photon states (photonic qubits) and continuous-variable (CV) of optical modes (photonic qumodes) plays important role in QI development. The one-way quantum computation (QC) based on multipartite cluster entanglement is initially proposed by Raussendorf and Briegel in the DV model [3], then it is extended to the CV regime by Menicucci et al [4]. For one-way QC model the qubits (qumodes) are initialized in a multipartite cluster entangled state firstly, then a variety of quantum logical operations can be achieved only via the single-qubit (qumode) projective measurement and the classical feedforward of the measured outcomes, in which the order and choices of measurements are determined by the required algorithm [3]. The basic logical operations of one-way DVQC has been experimentally demonstrated by several groups [5–7].

Parallely, the theoretical and experimental explorations on one-way CVQC were also proceeding continually [8–10, 12–15]. In contrast of the probabilistic generation of photonic qubits in most cases, CV cluster states are produced in an unconditional fashion and thus the one-way QC with CV cluster entangled photonic qumodes can be implemented deterministically [12–19]. Following the theoretical proposals on one-way CVQC the principally experimental demonstrations of various one-way QC logical operations over CVs were achieved by utilizing bipartite and four-partite cluster entangled photonic qumodes, respectively [12–15]. To develop more complicated QC larger cluster states with more numbers of entangled qubits (qumodes) are desired. However, the numbers of spatially separable entangled qumodes generated by experiments still stay below four-partites, so far [16–18]. In the paper, we present the first experimental achievement on producing CV eight-partite entangled states for photonic qumodes. Using eight squeezed states of light to be the initial resource quantum states and passing through the linearly optical transformation on a specially designed beam-splitter network, the eight-partite linear and two-diamond shape cluster states for photonic qumodes are prepared, respectively. The entanglement feature among the obtained eight space-separated photonic qumodes is confirmed by the fully inseparability criteria of CV multipartite entangled states proposed by van Loock and Furusawa [4].

The cluster state is a type of multipartite quantum entangled graph states corresponding to some mathematic graphs [2, 4, 10]. The CV cluster quadrature correlations (so-called nullifiers) can be expressed by [1, 2, 10]

$$(\hat{p}_a - \sum_{b \in N_a} \hat{x}_b) \rightarrow 0, \quad \forall \quad a \in G \quad (1)$$

where $\hat{x}_a = (\hat{a} + \hat{a}^\dagger)/2$ and $\hat{p}_a = (\hat{a} - \hat{a}^\dagger)/2i$ stand for quadrature-amplitude and quadrature-phase operators of an optical mode \hat{a} , respectively. The subscript a (b) expresses the designated mode \hat{a} (\hat{b}). The modes of $a \in G$ denote the vertices of the graph G , while the modes of $b \in N_a$ are the nearest neighbors of mode \hat{a} . For an ideal cluster state the left-hand side of equation (1) trends to zero, which stands for a simultaneous zero eigenstate of the quadrature combination [10]. The CV cluster quantum entanglements generated by experiments are deterministic, but also are imperfect, the entanglement features of which have to be verified and quantified by the sufficient conditions for the fully inseparability of multipartite CV entanglement [16–19]. There are different correlation combinations [left-hand side of equation (1)] in a variety of CV cluster multipartite entangled states, which reflect the complexity and rich

*Electronic address: kcpeng@sxu.edu.cn

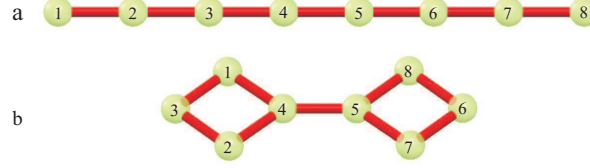


FIG. 1: The graph representation of eight-partite cluster states. a: linear cluster state, b: two-diamond shape cluster state. Each cluster node corresponds to an optical mode. The connected lines between neighboring nodes stand for the interaction among these nodes.

usability of these quantum systems. The expressions of the nullifiers for different graph states depend on their graph configurations.

Figure 1 (a) and (b) show the graph representations of CV eight-partite linear (a) and two-diamond (b) shape CV cluster states, respectively, each node of which corresponds to an optical mode and the connection lines between neighboring nodes stand for the interaction between the connected two nodes. From equation (1) and Fig. 1, we can write the nullifiers of the linear and the two-diamond shape CV cluster states, respectively, which are $\hat{p}_{L1} - \hat{x}_{L2} = \delta_{L1}$, $\hat{p}_{L2} - \hat{x}_{L1} - \hat{x}_{L3} = \delta_{L2}$, $\hat{p}_{L3} - \hat{x}_{L2} - \hat{x}_{L4} = \delta_{L3}$, $\hat{p}_{L4} - \hat{x}_{L3} - \hat{x}_{L5} = \delta_{L4}$, $\hat{p}_{L5} - \hat{x}_{L4} - \hat{x}_{L6} = \delta_{L5}$, $\hat{p}_{L6} - \hat{x}_{L5} - \hat{x}_{L7} = \delta_{L6}$, $\hat{p}_{L7} - \hat{x}_{L6} - \hat{x}_{L8} = \delta_{L7}$, $\hat{p}_{L8} - \hat{x}_{L7} = \delta_{L8}$ for the linear states; and $\hat{p}_{D1} - \hat{x}_{D3} - \hat{x}_{D4} = \delta_{D1}$, $\hat{p}_{D2} - \hat{x}_{D3} - \hat{x}_{D4} = \delta_{D2}$, $\hat{p}_{D3} - \hat{x}_{D1} - \hat{x}_{D2} = \delta_{D3}$, $\hat{p}_{D4} - \hat{x}_{D1} - \hat{x}_{D2} - \hat{x}_{D5} = \delta_{D4}$, $\hat{p}_{D5} - \hat{x}_{D4} - \hat{x}_{D7} - \hat{x}_{D8} = \delta_{D5}$, $\hat{p}_{D6} - \hat{x}_{D7} - \hat{x}_{D8} = \delta_{D6}$, $\hat{p}_{D7} - \hat{x}_{D5} - \hat{x}_{D6} = \delta_{D7}$, $\hat{p}_{D8} - \hat{x}_{D5} - \hat{x}_{D6} = \delta_{D8}$ for the two-diamond states, where the subscripts L_i and D_i ($i = 1, 2, \dots, 8$) denote the individual nodes of the linear and the two-diamond shape cluster states, respectively, δ_{L_i} and δ_{D_i} express the excess noises resulting from the imperfect quantum correlations. When the variance of δ_{L_i} (δ_{D_i}) is smaller than the corresponding quantum noise limit (QNL) determined by vacuum noises, the correlations among the combined optical modes is within the quantum region, otherwise the quantum correlations do not exist.

The schemes of generating CV multipartite entangled states commonly used in experiments are to achieve a linearly optical transformation of input squeezed states on a specific beam-splitter network [1]. Assuming \hat{a}_l and U_{kl} stand for the input squeezed states and the unitary matrix of a given beam-splitter network, respectively, the output optical modes after the transformation are given by $\hat{b}_k = \sum_l U_{kl} \hat{a}_l$, where the subscripts l and k express the designated input and output modes, respectively. In our experiment, four quadrature-amplitude \hat{x} -squeezed states, $\hat{a}_m = e^{-r} \hat{x}_m^{(0)} + ie^{+r} \hat{p}_m^{(0)}$ ($m = 1, 3, 5, 7$), and four quadrature-phase \hat{p} -squeezed states, $\hat{a}_n = e^{+r} \hat{x}_n^{(0)} + ie^{-r} \hat{p}_n^{(0)}$ ($n = 2, 4, 6, 8$), are applied, where $\hat{x}_j^{(0)}$ and $\hat{p}_j^{(0)}$ denote the quadrature-amplitude and the quadrature-phase operators of the corresponding vacuum field, respectively, r is the squeezing parameter to quantify the squeezing level, $r = 0$ and $r = +\infty$ correspond to the two cases of no squeezing and the ideally perfect squeezing, respectively. The unitary matrix for generating the CV eight-partite linear cluster state by combining eight squeezed states on optical beam splitters equals to (see Supplementary Material)

$$U_L = \begin{pmatrix} \frac{i}{\sqrt{2}} & \frac{i}{\sqrt{3}} & \frac{i}{\sqrt{10}} & \sqrt{\frac{3}{170}} & \sqrt{\frac{5}{102}} & 0 & 0 & 0 \\ \frac{-1}{\sqrt{2}} & \frac{1}{\sqrt{3}} & \frac{1}{\sqrt{10}} & -i\sqrt{\frac{3}{170}} & -i\sqrt{\frac{5}{102}} & 0 & 0 & 0 \\ 0 & \frac{i}{\sqrt{3}} & -i\sqrt{\frac{2}{5}} & -\sqrt{\frac{6}{85}} & -\sqrt{\frac{10}{51}} & 0 & 0 & 0 \\ 0 & 0 & \sqrt{\frac{2}{5}} & 3i\sqrt{\frac{3}{170}} & i\sqrt{\frac{15}{34}} & 0 & 0 & 0 \\ 0 & 0 & 0 & \sqrt{\frac{15}{34}} & -3\sqrt{\frac{3}{170}} & i\sqrt{\frac{2}{5}} & 0 & 0 \\ 0 & 0 & 0 & i\sqrt{\frac{10}{51}} & -i\sqrt{\frac{6}{85}} & \sqrt{\frac{2}{5}} & \frac{1}{\sqrt{3}} & 0 \\ 0 & 0 & 0 & -\sqrt{\frac{5}{102}} & \sqrt{\frac{3}{170}} & \frac{i}{\sqrt{10}} & \frac{-i}{\sqrt{3}} & \frac{-i}{\sqrt{2}} \\ 0 & 0 & 0 & -i\sqrt{\frac{5}{102}} & i\sqrt{\frac{3}{170}} & \frac{-1}{\sqrt{10}} & \frac{1}{\sqrt{3}} & \frac{-1}{\sqrt{2}} \end{pmatrix} \quad (2)$$

The unitary matrix in equation (2) expresses an optical transformation on a beam-splitter network consisting of seven beam splitters and can be decomposed into $U_L = F_8 I_7 (-1) F_6^\dagger F_4 I_3 (-1) F_2^\dagger B_{78}^-(1/2) F_8 B_{12}^-(1/2) F_1 B_{67}^-(1/3) F_7 B_{23}^-(1/3) F_2 B_{56}^-(2/5) F_6 B_{34}^-(2/5) F_3 B_{45}^+(25/34)$, where F_k denotes the Fourier transformation of mode k , which corresponds to a 90° rotation in the phase space; $B_{kl}^\pm(T_j)$ stands for the linearly optical transformation on the j th beam-splitter with the transmission of T_j ($j = 1, 2, 3, \dots, 7$),

where $(B_{kl}^\pm)_{kk} = \sqrt{1-T}$, $(B_{kl}^\pm)_{kl} = \sqrt{T}$, $(B_{kl}^\pm)_{lk} = \pm\sqrt{T}$, and $(B_{kl}^\pm)_{ll} = \mp\sqrt{1-T}$, are elements of beam-splitter matrix. $I_k(-1) = e^{i\pi}$ corresponds to a 180° rotation of mode k in the phase space.

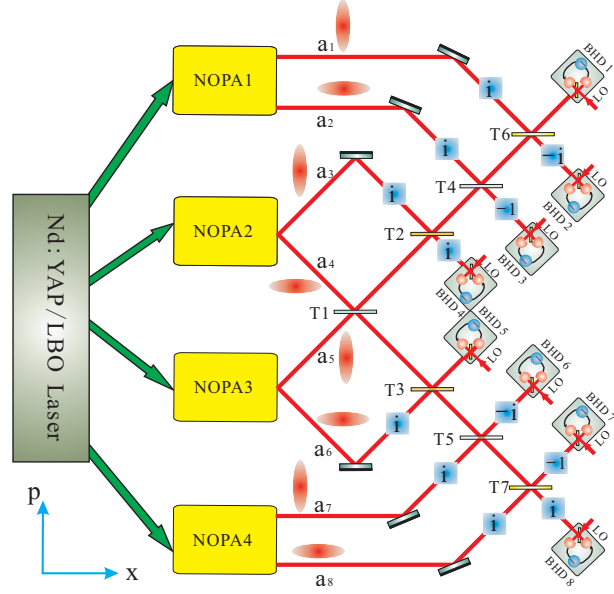


FIG. 2: Schematic of experimental setup for CV eight-partite cluster state generation. T : transmission efficient of beam splitter, Boxes including i are Fourier transforms (90° rotations in phase space), $-i$ is a -90° rotation, and -1 is a 180° rotation, BHD: balanced homodyne detector.

Figure 2 shows the schematic of the experimental set-up for preparing the eight-partite CV linear cluster state. The four \hat{x} -squeezed and four \hat{p} -squeezed states are produced by four NOPAs pumped by a common laser source, which is a CW intracavity frequency-doubled and frequency-stabilized Nd:YAP/LBO(Nd-doped YAlO_3 perovskite/lithium triborate) with both outputs of the fundamental and the second-harmonic waves [23]. The output fundamental wave at 1080 nm wavelength is used for the injected signals of NOPAs and the local oscillators of the balanced homodyne detectors (BHDs), which are applied to measure the quantum fluctuations of the quadrature-amplitude and the quadrature-phase of the output optical modes [16]. The second-harmonic wave at 540 nm wavelength serves as the pump field of the four NOPAs, in which through an intracavity frequency-down-conversion process a pair of signal and idler modes with the identical frequency at 1080 nm and the orthogonal polarizations are generated [5, 24]. Since the amplitude and the phase quadratures of the signal and the idler modes are entangled each other, the two coupled modes of them at $\pm 45^\circ$ polarization directions both are the squeezed states [7, 16]. In our experiment, the four NOPAs are operated at the parametric deamplification situation, i.e. the phase difference between the pump field and the injected signal is $(2n+1)\pi$ (n is an integer). Under this condition, the coupled modes at $+45^\circ$ and -45° polarization directions are the quadrature-amplitude and the quadrature-phase squeezed states, respectively [7, 16]. When the transmissions of the seven beam splitters are chosen as $T1 = 25/34$, $T2 = T3 = 2/5$, $T4 = T5 = 1/3$, $T6 = T7 = 1/2$, the eight output optical modes \hat{b}_j ($j = 1, 2, \dots, 8$) are in a eight-partite CV linear cluster state. The quadrature-amplitude and quadrature-phase of each \hat{b}_j are measured by eight BHDs, respectively. The nullifiers of the eight output modes depend on the squeezing parameters of the resource squeezed states. For our experimental system all four NOPAs have the identical configuration (the construction of NOPA is described in the Supplementary Material) and are operated under the same conditions. Each of NOPAs is also adjusted to produce two balanced squeezed states. So, the eight initial squeezed states own the same squeezed parameter r . In this case we can easily calculate the excess noises of the nullifiers for the eight-partite linear CV cluster state consisting of the eight output modes \hat{b}_j ($j = 1, \dots, 8$), which are $\delta_{L1} = \sqrt{2}e^{-r}\hat{x}_1^{(0)}$, $\delta_{L2} = \sqrt{3}e^{-r}\hat{p}_2^{(0)}$, $\delta_{L3} = \frac{1}{\sqrt{2}}e^{-r}\hat{x}_1^{(0)} - \sqrt{\frac{5}{2}}e^{-r}\hat{x}_3^{(0)}$, $\delta_{L4} = \frac{1}{\sqrt{3}}e^{-r}\hat{p}_2^{(0)} + \sqrt{\frac{2}{5}}e^{-r}\hat{p}_6^{(0)} + \sqrt{\frac{34}{15}}e^{-r}\hat{x}_5^{(0)}$, $\delta_{L5} = \sqrt{\frac{34}{15}}e^{-r}\hat{p}_4^{(0)} - \sqrt{\frac{2}{5}}e^{-r}\hat{x}_3^{(0)} - \frac{1}{\sqrt{3}}e^{-r}\hat{x}_7^{(0)}$, $\delta_{L6} = \sqrt{\frac{5}{2}}e^{-r}\hat{p}_6^{(0)} - \frac{1}{\sqrt{2}}e^{-r}\hat{p}_8^{(0)}$, $\delta_{L7} = -\sqrt{3}e^{-r}\hat{x}_7^{(0)}$ and $\delta_{L8} = -\sqrt{2}e^{-r}\hat{p}_8^{(0)}$, respectively.

The unitary matrix of the two-diamond cluster state U_D equals to $U_F U_L$, with $U_F = \text{diag}\{-1, -i, i, 1, 1, i, -i, -1\}$ (see Supplementary Material), thus the two-diamond shape cluster state can be prepared from the linear cluster state via local Fourier transforms and phase rotations. The excess noise terms of the nullifiers of the two-diamond shape

cluster state are expressed by $\delta_{D1} = -\frac{1}{\sqrt{2}}e^{-r}\hat{x}_1^{(0)} + \sqrt{\frac{5}{2}}e^{-r}\hat{x}_3^{(0)}$, $\delta_{D2} = \frac{1}{\sqrt{2}}e^{-r}\hat{x}_1^{(0)} - \sqrt{\frac{5}{2}}e^{-r}\hat{x}_3^{(0)}$, $\delta_{D3} = -\sqrt{3}e^{-r}\hat{p}_2^{(0)}$, $\delta_{D4} = -\frac{2}{\sqrt{3}}e^{-r}\hat{p}_2^{(0)} + \sqrt{\frac{2}{5}}e^{-r}\hat{p}_6^{(0)} + \sqrt{\frac{34}{15}}e^{-r}\hat{x}_5^{(0)}$, $\delta_{D5} = \sqrt{\frac{34}{15}}e^{-r}\hat{p}_4^{(0)} - \sqrt{\frac{2}{5}}e^{-r}\hat{x}_3^{(0)} + \frac{2}{\sqrt{3}}e^{-r}\hat{x}_7^{(0)}$, $\delta_{D6} = \sqrt{3}e^{-r}\hat{x}_7^{(0)}$, $\delta_{D7} = \sqrt{\frac{5}{2}}e^{-r}\hat{p}_6^{(0)} - \frac{1}{\sqrt{2}}e^{-r}\hat{p}_8^{(0)}$, and $\delta_{D8} = \sqrt{\frac{5}{2}}e^{-r}\hat{p}_6^{(0)} + \frac{1}{\sqrt{2}}e^{-r}\hat{p}_8^{(0)}$, respectively. According to the inseparability criteria for CV multipartite entangled states proposed by van Loock and Furusawa [4], we deduced the inseparability criterion inequalities for CV eight-partite linear and two-diamond shape cluster states, which are given by equations (3a)-(3g) and equations (4a)-(4i), respectively (see Supplementary Material).

$$V(\hat{p}_{L1} - \hat{x}_{L2}) + V(\hat{p}_{L2} - \hat{x}_{L1} - g_{L3}\hat{x}_{L3}) < 1 \quad (3a)$$

$$V(\hat{p}_{L2} - g_{L1}\hat{x}_{L1} - \hat{x}_{L3}) + V(\hat{p}_{L3} - \hat{x}_{L2} - g_{L4}\hat{x}_{L4}) < 1 \quad (3b)$$

$$V(\hat{p}_{L3} - g_{L2}\hat{x}_{L2} - \hat{x}_{L4}) + V(\hat{p}_{L4} - \hat{x}_{L3} - g_{L5}\hat{x}_{L5}) < 1 \quad (3c)$$

$$V(\hat{p}_{L4} - g_{L3}\hat{x}_{L3} - \hat{x}_{L5}) + V(\hat{p}_{L5} - \hat{x}_{L4} - g_{L6}\hat{x}_{L6}) < 1 \quad (3d)$$

$$V(\hat{p}_{L5} - g_{L4}\hat{x}_{L4} - \hat{x}_{L6}) + V(\hat{p}_{L6} - \hat{x}_{L5} - g_{L7}\hat{x}_{L7}) < 1 \quad (3e)$$

$$V(\hat{p}_{L6} - g_{L5}\hat{x}_{L5} - \hat{x}_{L7}) + V(\hat{p}_{L7} - \hat{x}_{L6} - g_{L8}\hat{x}_{L8}) < 1 \quad (3f)$$

$$V(\hat{p}_{L7} - g_{L6}\hat{x}_{L6} - \hat{x}_{L8}) + V(\hat{p}_{L8} - \hat{x}_{L7}) < 1 \quad (3g)$$

and

$$V(\hat{p}_{D1} - \hat{x}_{D3} - g_{D1}\hat{x}_{D4}) + V(\hat{p}_{D3} - \hat{x}_{D1} - g_{D2}\hat{x}_{D2}) < 1 \quad (4a)$$

$$V(\hat{p}_{D2} - \hat{x}_{D3} - g_{D1}\hat{x}_{D4}) + V(\hat{p}_{D3} - \hat{x}_{D2} - g_{D2}\hat{x}_{D1}) < 1 \quad (4b)$$

$$V(\hat{p}_{D1} - g_{D3}\hat{x}_{D3} - \hat{x}_{D4}) + V(\hat{p}_{D4} - \hat{x}_{D1} - g_{D4}\hat{x}_{D2} - g_{D5}\hat{x}_{D5}) < 1 \quad (4c)$$

$$V(\hat{p}_{D2} - g_{D3}\hat{x}_{D3} - \hat{x}_{D4}) + V(\hat{p}_{D4} - g_{D4}\hat{x}_{D1} - \hat{x}_{D2} - g_{D5}\hat{x}_{D5}) < 1 \quad (4d)$$

$$V(\hat{p}_{D4} - g_{D6}\hat{x}_{D1} - g_{D6}\hat{x}_{D2} - \hat{x}_{D5}) + V(\hat{p}_{D5} - \hat{x}_{D4} - g_{D6}\hat{x}_{D7} - g_{D6}\hat{x}_{D8}) < 1 \quad (4e)$$

$$V(\hat{p}_{D5} - g_{D5}\hat{x}_{D4} - \hat{x}_{D7} - g_{D4}\hat{x}_{D8}) + V(\hat{p}_{D7} - \hat{x}_{D5} - g_{D3}\hat{x}_{D6}) < 1 \quad (4f)$$

$$V(\hat{p}_{D5} - g_{D5}\hat{x}_{D4} - g_{D4}\hat{x}_{D7} - \hat{x}_{D8}) + V(\hat{p}_{D8} - \hat{x}_{D5} - g_{D3}\hat{x}_{D6}) < 1 \quad (4g)$$

$$V(\hat{p}_{D6} - \hat{x}_{D7} - g_{D2}\hat{x}_{D8}) + V(\hat{p}_{D7} - g_{D1}\hat{x}_{D5} - \hat{x}_{D6}) < 1 \quad (4h)$$

$$V(\hat{p}_{D6} - g_{D2}\hat{x}_{D7} - \hat{x}_{D8}) + V(\hat{p}_{D8} - g_{D1}\hat{x}_{D5} - \hat{x}_{D6}) < 1 \quad (4i)$$

where left-hand sides and right-hand sides of these inequalities are the combination of variances of nullifiers and the boundary, respectively. In the Supplementary Material, we numerically calculated the dependencies of the combinations of the correlation variances in the left-hand sides of equations (3) and equations (4) on the squeezing factor r for $g = 1$ and $g = g^{opt}$ (g^{opt} is the optimal gain factor), respectively. It can be seen, when the optimal gain factors are used the correlation variance combinations are always smaller than the boundary for all values of $r > 0$, i.e. the eight-partite CV cluster entanglement always can be realized by the presented system whatever how low the squeezing of the initial squeezed states is. However, when $g = 1$, a lower limitation of r is required to result in the correlation variances to be smaller than the boundary.

The experimentally measured initial squeezing degrees of the output fields from four NOPAs are 4.30 ± 0.07 dB below the QNL which corresponds to the squeezing parameter $r = 0.50 \pm 0.02$ (see Supplementary Material). During the measurements the pump power of NOPAs at 540 nm wavelength is ~ 180 mW, which is below the oscillation threshold of 240 mW, and the intensity of the injected signal at 1080 nm is 10 mW. The phase difference on each beam-splitters are locked according to the requirements. The light intensity of the local oscillator in all BHDs is set to around 5 mW. The measured QNL is about 20 dB above the electronics noise level, which guarantees that the results of the homodyne detections are almost not affected by electronic noises.

The correlation variances measured experimentally are shown in figure 3 for the linear cluster and figure 4 for the two-diamond cluster. They are $V(\hat{p}_{L1} - \hat{x}_{L2}) = -2.67 \pm 0.06$ dB, $V(\hat{p}_{L2} - \hat{x}_{L1} - \hat{x}_{L3}) = -2.65 \pm 0.13$ dB, $V(\hat{p}_{L3} - \hat{x}_{L2} - \hat{x}_{L4}) = -2.52 \pm 0.20$ dB, $V(\hat{p}_{L4} - \hat{x}_{L3} - \hat{x}_{L5}) = -2.69 \pm 0.09$ dB, $V(\hat{p}_{L5} - \hat{x}_{L4} - \hat{x}_{L6}) = -2.68 \pm 0.08$ dB, $V(\hat{p}_{L6} - \hat{x}_{L5} - \hat{x}_{L7}) = -2.56 \pm 0.10$ dB, $V(\hat{p}_{L7} - \hat{x}_{L6} - \hat{x}_{L8}) = -2.22 \pm 0.09$ dB, $V(\hat{p}_{L8} - \hat{x}_{L7}) = -2.21 \pm 0.09$ dB and $V(\hat{p}_{D1} - \hat{x}_{D3} - \hat{x}_{D4}) = -2.61 \pm 0.10$ dB, $V(\hat{p}_{D2} - \hat{x}_{D3} - \hat{x}_{D4}) = -2.57 \pm 0.09$ dB, $V(\hat{p}_{D3} - \hat{x}_{D1} - \hat{x}_{D2}) = -2.39 \pm 0.06$ dB, $V(\hat{p}_{D4} - \hat{x}_{D1} - \hat{x}_{D2} - \hat{x}_{D5}) = -2.58 \pm 0.09$ dB, $V(\hat{p}_{D5} - \hat{x}_{D4} - \hat{x}_{D7} - \hat{x}_{D8}) = -2.61 \pm 0.09$ dB, $V(\hat{p}_{D6} - \hat{x}_{D7} - \hat{x}_{D8}) = -2.52 \pm 0.10$ dB, $V(\hat{p}_{D7} - \hat{x}_{D5} - \hat{x}_{D6}) = -2.59 \pm 0.09$ dB, $V(\hat{p}_{D8} - \hat{x}_{D5} - \hat{x}_{D6}) = -2.58 \pm 0.10$ dB, $V(\hat{p}_{D4} - g_{D6}\hat{x}_{D1} - g_{D6}\hat{x}_{D2} - \hat{x}_{D5}) = -1.57 \pm 0.09$ dB, $V(\hat{p}_{D5} - \hat{x}_{D4} - g_{D6}\hat{x}_{D7} - g_{D6}\hat{x}_{D8}) = -1.53 \pm 0.09$ dB. From these measured results we can calculate the combinations of the correlation variances in the left-hand sides of the inequalities (3a)-(3g) and (4a)-(4i), which are 0.68 ± 0.02 , 0.83 ± 0.02 , 0.82 ± 0.02 , 0.81 ± 0.02 , 0.82 ± 0.02 , 0.87 ± 0.02 , 0.75 ± 0.02 , for the linear cluster and 0.84 ± 0.02 , 0.85 ± 0.02 , 0.96 ± 0.02 , 0.97 ± 0.02 , 0.95 ± 0.02 ,

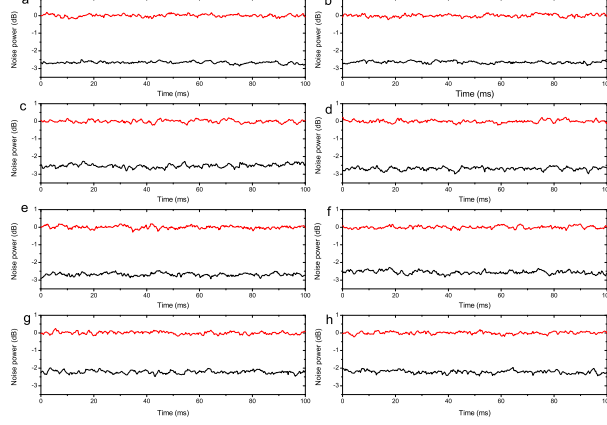


FIG. 3: The measured noise powers of eight-partite linear cluster state. The upper and lower lines in all graphs are shot noise level and correlation variances of nullifiers, respectively. (a)-(h) are noise powers of $V(\hat{p}_{L1} - \hat{x}_{L2})$, $V(\hat{p}_{L2} - \hat{x}_{L1} - \hat{x}_{L3})$, $V(\hat{p}_{L3} - \hat{x}_{L2} - \hat{x}_{L4})$, $V(\hat{p}_{L4} - \hat{x}_{L3} - \hat{x}_{L5})$, $V(\hat{p}_{L5} - \hat{x}_{L4} - \hat{x}_{L6})$, $V(\hat{p}_{L6} - \hat{x}_{L5} - \hat{x}_{L7})$, $V(\hat{p}_{L7} - \hat{x}_{L6} - \hat{x}_{L8})$, and $V(\hat{p}_{L8} - \hat{x}_{L7})$, respectively. The measurement frequency is 2 MHz, resolution bandwidth is 30 kHz, and video bandwidth is 100 Hz.

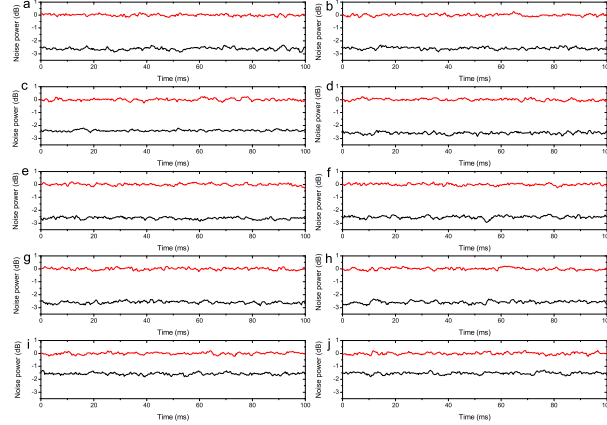


FIG. 4: The measured noise powers of eight-partite two-diamond shape cluster state. The upper and lower lines in all graphs are shot noise level and correlation variances of nullifiers, respectively. (a)-(j) are noise powers of $V(\hat{p}_{D1} - \hat{x}_{D3} - \hat{x}_{D4})$, $V(\hat{p}_{D2} - \hat{x}_{D3} - \hat{x}_{D4})$, $V(\hat{p}_{D3} - \hat{x}_{D1} - \hat{x}_{D2})$, $V(\hat{p}_{D4} - \hat{x}_{D1} - \hat{x}_{D2} - \hat{x}_{D5})$, $V(\hat{p}_{D5} - \hat{x}_{D4} - \hat{x}_{D7} - \hat{x}_{D8})$, $V(\hat{p}_{D6} - \hat{x}_{D7} - \hat{x}_{D8})$, $V(\hat{p}_{D7} - \hat{x}_{D5} - \hat{x}_{D6})$, $V(\hat{p}_{D8} - \hat{x}_{D5} - \hat{x}_{D6})$, $V(\hat{p}_{D4} - g_{D6}\hat{x}_{D1} - g_{D6}\hat{x}_{D2} - \hat{x}_{D5})$, $V(\hat{p}_{D5} - \hat{x}_{D4} - g_{D6}\hat{x}_{D7} - g_{D6}\hat{x}_{D8})$, respectively. The measurement frequency is 2 MHz, resolution bandwidth is 30 kHz, and video bandwidth is 100 Hz.

0.96 ± 0.02 , 0.96 ± 0.02 , 0.83 ± 0.02 , 0.83 ± 0.02 for the two-diamond cluster, respectively. All these values are smaller than the boundary. It means that the prepared two types of CV cluster states satisfy the inseparability criteria for verifying multipartite CV entanglement, so the spatially separated eight-partite entangled states of photonic qumodes are experimentally obtained. In the experiment we detected the correlation variances under $g_{L1-L8} = 1$, $g_{D1-D5} = 1$ and $g_{D6} = g_{D6}^{opt} = 0.60 \pm 0.02$. For our system, the total transmission efficiency of squeezed beams are about 87% and the detection efficiency is about 90%, which lead to the efficient squeezing parameter is $r_e = 0.30$ which is smaller than the initially measured squeezing parameter. When the gain factors except g_{D6} are taken as 1 and only g_{D6}^{opt} is utilized, all inequalities in equation (3) and equation (4) are satisfied. If $r_e > 0.35$, the unite gain factor of $g_{D6} = 1$ can be chosen also (see Supplementary Material).

In the conclusion, we have experimentally prepared two types of spatially separated eight-partite CV cluster entan-

gled states for photonic qumodes by using eight quadrature squeezed states of light and a specifically designed optical beam-splitter network. The multipartite entangled states are the essential resources to construct a variety of CVQI networks. So far, the single-mode squeezed states over 12.7 dB [27] and the two-mode squeezed states over 8.1 dB [28] have been experimentally generated, respectively, based on which and using the presented scheme the CV cluster states with more space-separable qumodes and higher entanglement can be obtained. The complexity and versatility of CV multipartite entanglement for photonic qumodes not only offer richly potential applications in QC and QI, but also provide the basic and handleable entangled quantum states which can be an important tool for further studying the amazing and attractive quantum entanglement phenomena.

This research was supported by the National Basic Research Program of China (Grant No. 2010CB923103) and NSFC (Grant Nos. 11174188, 61121064).

-
- [1] M. A. Nielsen and I. L. Chuang, *Quantum computation and quantum information* (Cambridge University Press, Cambridge, 2000).
 - [2] S. L. Braunstein and P. van Loock, *Rev. Mod. Phys.* **77**, 513-577 (2005).
 - [3] R. Raussendorf, and H. J. Briegel, *Phys. Rev. Lett.* **86**, 5188-5191 (2001).
 - [4] N. C. Menicucci, *et al.* *Phys. Rev. Lett.* **97**, 110501 (2006).
 - [5] P. Walther, *et al.* *Nature* **434**, 169-176 (2005).
 - [6] K. Chen, *et al.* *Phys. Rev. Lett.* **99**, 120503 (2007).
 - [7] W.-B. Gao, *et al.* *Phys. Rev. Lett.* **104**, 020501 (2010).
 - [8] P. van Loock, *J. Opt. Soc. Am. B* **24**, 340-346 (2007).
 - [9] A. Tan, C. Xie, and K. Peng, *Phys. Rev. A* **79**, 042338 (2009).
 - [10] M. Gu, C. Weedbrook, N. C. Menicucci, T. C. Ralph, and P. van Loock, *Phys. Rev. A* **79**, 062318 (2009).
 - [11] H. Yonezawa, T. Aoki and A. Furusawa, *Nature* **431**, 430-433 (2004).
 - [12] Y. Miwa, J. I. Yoshikawa, P. van Loock, and A. Furusawa, *Phys. Rev. A* **80**, 050303(R) (2009).
 - [13] Y. Wang, *et al.* *Phys. Rev. A* **81**, 022311 (2010).
 - [14] R. Ukai, *et al.* *Phys. Rev. Lett.* **106**, 240504 (2011).
 - [15] R. Ukai, S. Yokoyama, J. I. Yoshikawa, P. van Loock, and A. Furusawa, *Phys. Rev. Lett.* **107**, 250501 (2011).
 - [16] X. Su, *et al.* *Phys. Rev. Lett.* **98**, 070502 (2007).
 - [17] M. Yukawa, R. Ukai, P. van Loock, and A. Furusawa, *Phys. Rev. A* **78**, 012301 (2008).
 - [18] A. Tan, *et al.* *Phys. Rev. A* **78**, 013828 (2008).
 - [19] M. Pysher, Y. Miwa, R. Shahrokhshahi, R. Bloomer, and O. Pfister, *Phys. Rev. Lett.* **107**, 030505 (2011).
 - [20] P. van Loock and A. Furusawa, *Phys. Rev. A* **67**, 052315 (2003).
 - [21] J. Zhang and S. L. Braunstein, *Phys. Rev. A* **73**, 032318 (2006).
 - [22] P. van Loock, C. Weedbrook, and M. Gu, *Phys. Rev. A* **76**, 032321 (2007).
 - [23] Y. Wang, Y. Zheng, C. Xie, and K. Peng, *IEEE J. Quantum Electronics* **47**, (7), 1006 (2011).
 - [24] X. Li, *et al.* *Phys. Rev. Lett.* **88**, 047904 (2002).
 - [25] Y. Wang, *et al.* *Opt. Express* **18**, 6149-6155 (2010).
 - [26] Y. Zhang, *et al.* *Phys. Rev. A* **62**, 023813 (2000).
 - [27] T. Eberle, *et al.* *Phys. Rev. Lett.* **104**, 251102 (2010).
 - [28] Z. Yan, *et al.* *Phys. Rev. A* **85**, 040305(R) (2012).

Supplementary Information for “Experimental preparation of eight-partite linear and two-diamond shape cluster states for photonic qumodes”

Xiaolong Su, Yaping Zhao, Shuhong Hao, Xiaojun Jia, Changde Xie, and Kunchi Peng*
 State Key Laboratory of Quantum Optics and Quantum Optics Devices, Institute of Opto-Electronics, Shanxi
 University, Taiyuan, 030006, People’s Republic of China
 *e-mail:kcpeng@sxu.edu.cn

I. UNITARY MATRIX FOR GENERATING CV EIGHT-PARTITE CLUSTER STATES

According to the proposal of Peter van Loock et al [1], CV cluster states of photonic qumodes can be created via a general linear-optics transformation of \hat{p} -squeezed input modes. If $\hat{a}_l = e^{+r}\hat{x}_l^{(0)} + ie^{-r}\hat{p}_l^{(0)}$ and a unitary matrix U stand for the annihilation operator of the input modes and the linear-optical transformation respectively, the output modes after the transformation are expressed by $\hat{b}_k = \sum_l U_{kl}\hat{a}_l$, which are the CV cluster states [1, 2]. The CV cluster states satisfy $I\text{Im}[UB_{in}] - A\text{Re}[UB_{in}] \rightarrow 0$ in the limit of infinite squeezing, where I is the identity matrix, $B_{in} = (\hat{a}_1, \hat{a}_2, \dots, \hat{a}_n)^T$ is the matrix of input states, A is the adjacency matrix [3]. So we have $I\text{Im}U = A\text{Re}U$, and the unitary matrix is obtained

$$U = (I + iA)\text{Re}U. \quad (5)$$

Based on the unitarity of matrix U , $UU^\dagger = I$, we have

$$\text{Re}U(\text{Re}U)^T = (I + A^2)^{-1}. \quad (6)$$

In this case, we can obtain $\text{Re}U$ and U from the adjacency matrix A .

For n -partite cluster state, assuming

$$\text{Re}U = \begin{pmatrix} \vec{\alpha}_1^T \\ \vec{\alpha}_2^T \\ \vdots \\ \vec{\alpha}_n^T \end{pmatrix} \quad (7)$$

where $\vec{\alpha}_i^T = (\alpha_{i1}, \alpha_{i2}, \dots, \alpha_{in})$ is a real vectors. According to Eq. (2), we have $\vec{\alpha}_i^T \vec{\alpha}_j = (I + A^2)^{-1}_{ij}$ ($i, j = 1, \dots, n$), where the numbers of these equations are $n(n+1)/2$ according to the symmetry of matrix. Since there are n^2 unknown numbers in all these equations, we need $n(n-1)/2$ conditions to solve the equations. For simplicity and without lossing generality, some unknown numbers in the equations are chosen to be 0 when we solve the equations.

For CV eight-partite linear cluster state, the adjacency matrix can be written as

$$A = \begin{pmatrix} 0 & 1 & 0 & 0 & 0 & 0 & 0 & 0 \\ 1 & 0 & 1 & 0 & 0 & 0 & 0 & 0 \\ 0 & 1 & 0 & 1 & 0 & 0 & 0 & 0 \\ 0 & 0 & 1 & 0 & 1 & 0 & 0 & 0 \\ 0 & 0 & 0 & 1 & 0 & 1 & 0 & 0 \\ 0 & 0 & 0 & 0 & 1 & 0 & 1 & 0 \\ 0 & 0 & 0 & 0 & 0 & 1 & 0 & 1 \\ 0 & 0 & 0 & 0 & 0 & 0 & 1 & 0 \end{pmatrix} \quad (8)$$

we have

$$(I + A^2)^{-1} = \begin{pmatrix} \frac{21}{34} & 0 & -\frac{4}{17} & 0 & \frac{3}{34} & 0 & -\frac{1}{34} & 0 \\ 0 & \frac{13}{34} & 0 & \frac{5}{34} & 0 & \frac{1}{17} & 0 & -\frac{1}{34} \\ -\frac{4}{17} & 0 & \frac{8}{17} & 0 & -\frac{3}{17} & 0 & \frac{1}{17} & 0 \\ 0 & \frac{5}{34} & 0 & \frac{15}{34} & 0 & -\frac{3}{17} & 0 & \frac{3}{34} \\ \frac{3}{34} & 0 & -\frac{3}{17} & 0 & \frac{15}{34} & 0 & -\frac{5}{34} & 0 \\ 0 & \frac{1}{17} & 0 & -\frac{3}{17} & 0 & \frac{8}{17} & 0 & -\frac{4}{17} \\ -\frac{1}{34} & 0 & \frac{1}{17} & 0 & -\frac{5}{34} & 0 & \frac{13}{34} & 0 \\ 0 & -\frac{1}{34} & 0 & \frac{3}{34} & 0 & -\frac{4}{17} & 0 & \frac{21}{34} \end{pmatrix} \quad (9)$$

The matrix elements in Eq. (3) are obtained by the following way. Considering the symmetry, we start from the middle row, $\vec{\alpha}_4^T = (\alpha_{41}, \alpha_{42}, \alpha_{43}, \alpha_{44}, \alpha_{45}, \alpha_{46}, \alpha_{47}, \alpha_{48})$. We apply seven initial conditions, $\alpha_{41} = \alpha_{42} = \alpha_{43} = \alpha_{44} = \alpha_{46} = \alpha_{47} = \alpha_{48} = 0$, then it becomes $\vec{\alpha}_4^T = (0 \ 0 \ 0 \ 0 \ \alpha_{45} \ 0 \ 0 \ 0)$. According to equations $\vec{\alpha}_4^T \vec{\alpha}_4 = (I + A^2)_{44}^{-1} = \frac{15}{34}$, first unknown number $\alpha_{45} = -\sqrt{\frac{15}{34}}$ is obtained. Then we apply six conditions, $\alpha_{51} = \alpha_{52} = \alpha_{53} = \alpha_{56} = \alpha_{57} = \alpha_{58} = 0$ on $\vec{\alpha}_5^T$, we have $\vec{\alpha}_5^T = (0 \ 0 \ 0 \ \alpha_{54} \ \alpha_{55} \ 0 \ 0 \ 0)$. Using equations $\vec{\alpha}_5^T \vec{\alpha}_5 = (I + A^2)_{55}^{-1} = \frac{15}{34}$ and $\alpha_5^T \alpha_4 = (I + A^2)_{54}^{-1} = 0$, two unknown numbers $\alpha_{55} = 0$, $\alpha_{54} = -\sqrt{\frac{15}{34}}$ are gotten, and so on.

After all the unknown numbers in Eq. (3) are obtained, the unitary matrix is given from Eq. (1). The unitary matrix for eight-partite linear cluster state with eight \hat{p} -squeezed states to be the input states are expressed

$$U_L^p = \begin{pmatrix} \frac{1}{\sqrt{2}} & \frac{i}{\sqrt{3}} & \frac{1}{\sqrt{10}} & -\sqrt{\frac{3}{170}} & i\sqrt{\frac{5}{102}} & 0 & 0 & 0 \\ \frac{i}{\sqrt{2}} & \frac{1}{\sqrt{3}} & \frac{-i}{\sqrt{10}} & i\sqrt{\frac{3}{170}} & \sqrt{\frac{5}{102}} & 0 & 0 & 0 \\ 0 & \frac{i}{\sqrt{3}} & -\sqrt{\frac{2}{5}} & \sqrt{\frac{6}{85}} & -i\sqrt{\frac{10}{51}} & 0 & 0 & 0 \\ 0 & 0 & -i\sqrt{\frac{2}{5}} & -3i\sqrt{\frac{3}{170}} & -\sqrt{\frac{15}{34}} & 0 & 0 & 0 \\ 0 & 0 & 0 & -\sqrt{\frac{15}{34}} & -3i\sqrt{\frac{3}{170}} & i\sqrt{\frac{2}{5}} & 0 & 0 \\ 0 & 0 & 0 & -i\sqrt{\frac{10}{51}} & \sqrt{\frac{6}{85}} & \sqrt{\frac{2}{5}} & \frac{i}{\sqrt{3}} & 0 \\ 0 & 0 & 0 & \sqrt{\frac{3}{170}} & i\sqrt{\frac{5}{102}} & \frac{i}{\sqrt{10}} & \frac{1}{\sqrt{3}} & \frac{-i}{\sqrt{2}} \\ 0 & 0 & 0 & i\sqrt{\frac{5}{102}} & -\sqrt{\frac{3}{170}} & \frac{-1}{\sqrt{10}} & \frac{i}{\sqrt{3}} & \frac{-1}{\sqrt{2}} \end{pmatrix} \quad (10)$$

In the experiment, we prepared four \hat{x} -squeezed states, $\hat{a}_m = e^{-r}\hat{x}_m^{(0)} + ie^{+r}\hat{p}_m^{(0)}$ ($m = 1, 3, 5, 7$), and four \hat{p} -squeezed states, $\hat{a}_n = e^{+r}\hat{x}_n^{(0)} + ie^{-r}\hat{p}_n^{(0)}$ ($n = 2, 4, 6, 8$) with four NOPAs, respectively. The transformation between \hat{x} -squeezed state and \hat{p} -squeezed state can be achieved via a Fourier transformation. Applying Fourier transformation on modes $\hat{a}_1, \hat{a}_3, \hat{a}_5$ and \hat{a}_7 , which corresponds to multiplying i to the values of columns 1, 3, 5 and 7 in the unitary matrix U_L^p , we obtain the unitary matrix of CV eight-partite linear cluster state for our experimental system, which is

$$U_L = \begin{pmatrix} \frac{i}{\sqrt{2}} & \frac{i}{\sqrt{3}} & \frac{i}{\sqrt{10}} & \sqrt{\frac{3}{170}} & \sqrt{\frac{5}{102}} & 0 & 0 & 0 \\ \frac{-1}{\sqrt{2}} & \frac{1}{\sqrt{3}} & \frac{1}{\sqrt{10}} & -i\sqrt{\frac{3}{170}} & -i\sqrt{\frac{5}{102}} & 0 & 0 & 0 \\ 0 & \frac{i}{\sqrt{3}} & -i\sqrt{\frac{2}{5}} & -\sqrt{\frac{6}{85}} & -\sqrt{\frac{10}{51}} & 0 & 0 & 0 \\ 0 & 0 & \sqrt{\frac{2}{5}} & 3i\sqrt{\frac{3}{170}} & i\sqrt{\frac{15}{34}} & 0 & 0 & 0 \\ 0 & 0 & 0 & \sqrt{\frac{15}{34}} & -3i\sqrt{\frac{3}{170}} & i\sqrt{\frac{2}{5}} & 0 & 0 \\ 0 & 0 & 0 & i\sqrt{\frac{10}{51}} & -i\sqrt{\frac{6}{85}} & \sqrt{\frac{2}{5}} & \frac{1}{\sqrt{3}} & 0 \\ 0 & 0 & 0 & -\sqrt{\frac{3}{170}} & \sqrt{\frac{5}{102}} & \frac{i}{\sqrt{10}} & \frac{-i}{\sqrt{3}} & \frac{-i}{\sqrt{2}} \\ 0 & 0 & 0 & -i\sqrt{\frac{5}{102}} & i\sqrt{\frac{3}{170}} & \frac{-1}{\sqrt{10}} & \frac{1}{\sqrt{3}} & \frac{-1}{\sqrt{2}} \end{pmatrix} \quad (11)$$

Similarly, the unitary matrix for generating CV eight-partite two-diamond shape cluster state can be obtained with the same way. The calculated results show that U_D equals to $U_F U_L$, where $U_F = \text{diag}\{-1, -i, i, 1, 1, i, -i, -1\}$. The unitary matrix U_D is given by

$$U_D = \begin{pmatrix} \frac{-i}{\sqrt{2}} & \frac{-i}{\sqrt{3}} & \frac{-i}{\sqrt{10}} & -\sqrt{\frac{3}{170}} & -\sqrt{\frac{5}{102}} & 0 & 0 & 0 \\ \frac{i}{\sqrt{2}} & \frac{-i}{\sqrt{3}} & \frac{-i}{\sqrt{10}} & -\sqrt{\frac{3}{170}} & -\sqrt{\frac{5}{102}} & 0 & 0 & 0 \\ 0 & \frac{-1}{\sqrt{3}} & \sqrt{\frac{2}{5}} & -i\sqrt{\frac{6}{85}} & -i\sqrt{\frac{10}{51}} & 0 & 0 & 0 \\ 0 & 0 & \sqrt{\frac{2}{5}} & 3i\sqrt{\frac{3}{170}} & i\sqrt{\frac{15}{34}} & 0 & 0 & 0 \\ 0 & 0 & 0 & \sqrt{\frac{15}{34}} & -3\sqrt{\frac{3}{170}} & i\sqrt{\frac{2}{5}} & 0 & 0 \\ 0 & 0 & 0 & -\sqrt{\frac{10}{51}} & \sqrt{\frac{6}{85}} & i\sqrt{\frac{2}{5}} & \frac{i}{\sqrt{3}} & 0 \\ 0 & 0 & 0 & i\sqrt{\frac{5}{102}} & -i\sqrt{\frac{3}{170}} & \frac{1}{\sqrt{10}} & \frac{-1}{\sqrt{3}} & \frac{-1}{\sqrt{2}} \\ 0 & 0 & 0 & i\sqrt{\frac{5}{102}} & -i\sqrt{\frac{3}{170}} & \frac{1}{\sqrt{10}} & \frac{-1}{\sqrt{3}} & \frac{1}{\sqrt{2}} \end{pmatrix} \quad (12)$$

II. INSEPARABILITY CRITERIA

According to the inseparability criteria for CV multipartite entangled states proposed by van Loock and Furusawa [4], we deduced the concrete inseparability conditions for CV eight-partite linear cluster state, which are Eqs. (3) in the main text. For any separable quantum state, its total density operator can be written as $\hat{\rho} = \sum_i \eta_i \hat{\rho}_{i,k,\dots,m} \otimes \hat{\rho}_{i,l,\dots,n}$ with a distinct pair of “separable modes” (m, n) and the other modes $k \neq l$ [see equation (25) in Ref. 2.], where η_i represent the mixture of these separable states. For any combinations $\hat{u} = h_1 \hat{x}_1 + h_2 \hat{x}_2 + \dots + h_N \hat{x}_N$ and $\hat{v} = g_1 \hat{p}_1 + g_2 \hat{p}_2 + \dots + g_N \hat{p}_N$, the inseparability criteria are expressed by [4]

$$V(\hat{u}) + V(\hat{v}) < \frac{1}{2} \left(\left| h_m g_m + \sum_k h_k g_k \right| + \left| h_n g_n + \sum_l h_l g_l \right| \right) \quad (13)$$

Based on this equation, we deduced the inseparability criteria for CV eight-partite linear and two-diamond shape cluster states, which are Eqs. (3) and (4) in the main text, respectively.

The violation of each inequality in Eqs. (3) can be used to verify variously partially separable states, that are

$$\begin{aligned} \text{violation of (3a)} &\implies \hat{\rho} = \sum_i \eta_i \hat{\rho}_{i,k,\dots,1} \otimes \hat{\rho}_{i,l,\dots,2} \\ \text{violation of (3b)} &\implies \hat{\rho} = \sum_i \eta_i \hat{\rho}_{i,k,\dots,2} \otimes \hat{\rho}_{i,l,\dots,3} \\ \text{violation of (3c)} &\implies \hat{\rho} = \sum_i \eta_i \hat{\rho}_{i,k,\dots,3} \otimes \hat{\rho}_{i,l,\dots,4} \\ \text{violation of (3d)} &\implies \hat{\rho} = \sum_i \eta_i \hat{\rho}_{i,k,\dots,4} \otimes \hat{\rho}_{i,l,\dots,5} \\ \text{violation of (3e)} &\implies \hat{\rho} = \sum_i \eta_i \hat{\rho}_{i,k,\dots,5} \otimes \hat{\rho}_{i,l,\dots,6} \\ \text{violation of (3f)} &\implies \hat{\rho} = \sum_i \eta_i \hat{\rho}_{i,k,\dots,6} \otimes \hat{\rho}_{i,l,\dots,7} \\ \text{violation of (3g)} &\implies \hat{\rho} = \sum_i \eta_i \hat{\rho}_{i,k,\dots,7} \otimes \hat{\rho}_{i,l,\dots,8} \end{aligned} \quad (14)$$

If all inequalities in Eqs. (3) are satisfied, we can confirm that all eight states are inseparable and thus they construct a CV eight-partite linear cluster entangled state.

We also deduced the inseparability criteria for CV eight-partite two-diamond shape linear cluster state, which are Eqs. (4) in the main text. Similarly, if the inequalities are violated the partially separable states are expressed by

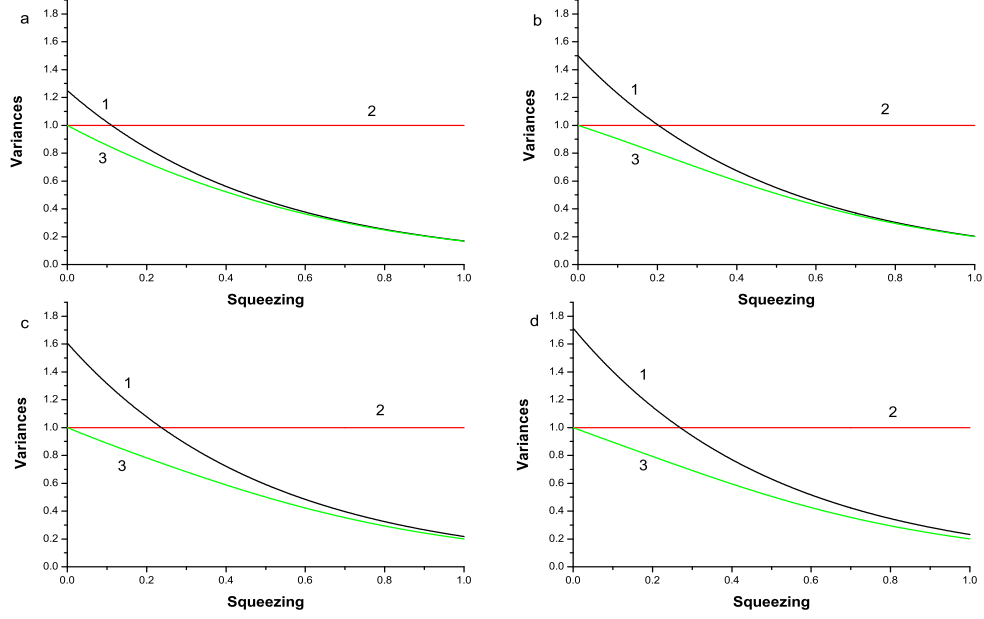


FIG. 5: The dependence of eight-partite linear cluster state to squeezing parameter, a-d are corresponding to inequalities (3a)-(3d), respectively. Lines 1 and 3 are left-hand sides of inequalities with unit gain and optimal gain, respectively, line 2 are right-hand sides of inequalities.

$$\begin{aligned}
 \text{violation of (4a)} &\implies \hat{\rho} = \sum_i \eta_i \hat{\rho}_{i,k,\dots,1} \otimes \hat{\rho}_{i,l,\dots,3} \\
 \text{violation of (4b)} &\implies \hat{\rho} = \sum_i \eta_i \hat{\rho}_{i,k,\dots,2} \otimes \hat{\rho}_{i,l,\dots,3} \\
 \text{violation of (4c)} &\implies \hat{\rho} = \sum_i \eta_i \hat{\rho}_{i,k,\dots,1} \otimes \hat{\rho}_{i,l,\dots,4} \\
 \text{violation of (4d)} &\implies \hat{\rho} = \sum_i \eta_i \hat{\rho}_{i,k,\dots,2} \otimes \hat{\rho}_{i,l,\dots,4} \\
 \text{violation of (4e)} &\implies \hat{\rho} = \sum_i \eta_i \hat{\rho}_{i,k,\dots,4} \otimes \hat{\rho}_{i,l,\dots,5} \\
 \text{violation of (4f)} &\implies \hat{\rho} = \sum_i \eta_i \hat{\rho}_{i,k,\dots,5} \otimes \hat{\rho}_{i,l,\dots,7} \\
 \text{violation of (4g)} &\implies \hat{\rho} = \sum_i \eta_i \hat{\rho}_{i,k,\dots,5} \otimes \hat{\rho}_{i,l,\dots,8} \\
 \text{violation of (4h)} &\implies \hat{\rho} = \sum_i \eta_i \hat{\rho}_{i,k,\dots,6} \otimes \hat{\rho}_{i,l,\dots,7} \\
 \text{violation of (4i)} &\implies \hat{\rho} = \sum_i \eta_i \hat{\rho}_{i,k,\dots,6} \otimes \hat{\rho}_{i,l,\dots,8}
 \end{aligned} \tag{15}$$

When all inequalities in Eqs. (4) are satisfied CV eight-partite two-diamond shape cluster entanglement is demonstrated.

Calculating the minimal values of the left-hand sides of the inequalities versus the gain factors (g_{L1-L8} for the linear shape and g_{D1-D6} for the two-diamond shape) we can obtain the optimal gain factors g_{L1-L8}^{opt} and g_{D1-D6}^{opt} for achieving the detections of the minimal correlation variances. For the linear (g_{L1-L8}^{opt}) and the two diamond (g_{D1-D6}^{opt}) cluster states the optimal gain factors are $g_{L1} = g_{L8} = \frac{21(e^{4r}-1)}{13+21e^{4r}}$, $g_{L2} = g_{L7} = \frac{13(e^{4r}-1)}{21+13e^{4r}}$, $g_{L3} = g_{L6} = \frac{8(e^{4r}-1)}{9+8e^{4r}}$, $g_{L4} = g_{L5} = \frac{15(e^{4r}-1)}{19+15e^{4r}}$ and $g_{D1} = \frac{15(e^{4r}-1)}{19+15e^{4r}}$, $g_{D2} = \frac{21(e^{4r}-1)}{13+21e^{4r}}$, $g_{D3} = \frac{9(e^{4r}-1)}{8+9e^{4r}}$, $g_{D4} = \frac{9(e^{8r}-1)}{7+18e^{4r}+9e^{8r}}$, $g_{D5} = \frac{3(3e^{8r}-2e^{4r}-1)}{7+18e^{4r}+9e^{8r}}$, $g_{D6} = \frac{4(e^{4r}-1)}{13+4e^{4r}}$, respectively. The dependence of inseparability criteria of CV eight-partite linear cluster state on the

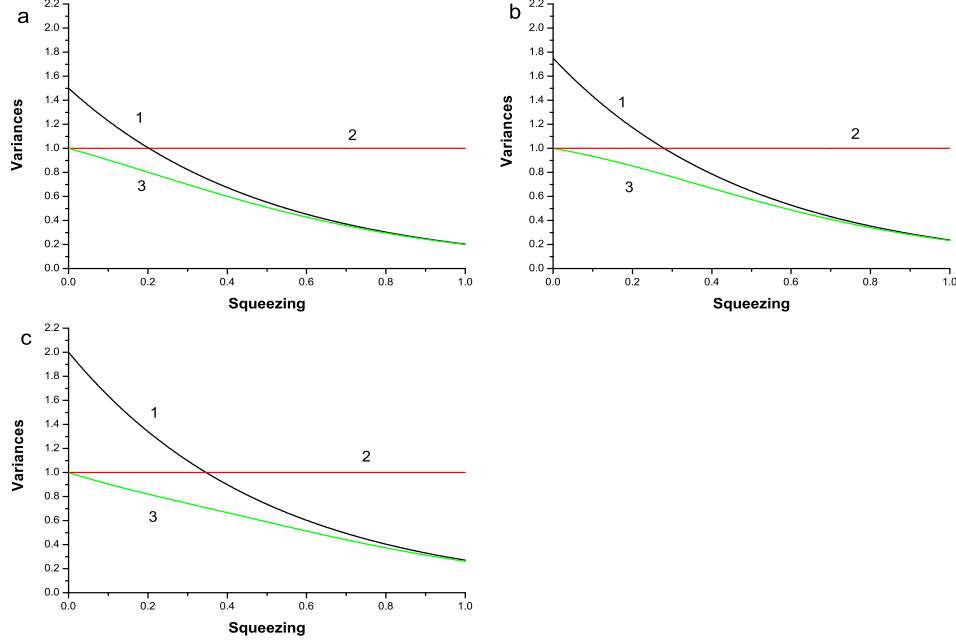


FIG. 6: The dependence of eight-partite two-diamond shape cluster state to squeezing parameter, a, b and c are corresponding to inequalities (4a), (4c), and (4e), respectively. Lines 1 and 3 are left-hand sides of inequalities with unit gain and optimal gain, respectively, line 2 are right-hand sides of inequalities.

squeezing parameter is shown in figure 1. In Fig. 1, (a), (b), (c) and (d) correspond to inequalities (3a), (3b), (3c) and (3d), respectively. Lines 1 and 3 are the variance combinations in the left-hand sides of inequalities with unit gain and the optimal gain, respectively. Line 2 stands for the boundary corresponding to right-hand sides of inequalities. Since the other inequalities have same variances with (3a)-(3c), we only show the four results here. For inequalities (3a)-(3d), if the unit gain factor is used only when $r > 0.11$, $r > 0.20$, $r > 0.24$, and $r > 0.27$ these inequalities are satisfied. However, if the optimal gain factors are chosen, these criterion inequalities are always satisfied for any $r > 0$, i.e. the presented system can prepare the CV eight-partite cluster state without the lower limitation of the squeezing degree for the input squeezed state.

The dependence of inseparability criteria of CV eight-partite two-diamond shape cluster state to the squeezing parameter is shown in figure 2. Since the variances of inequalities (4a), (4b), (4h) and (4i) are the same, and that of (4c), (4d), (4f) and (4g) are also the same, we only plot the correlation variances of the inequalities (4a), (4c) and (4e) in Fig. 2a, 2b and 2c, respectively. From Fig. 2a, 2b and 2c, we can see that when the squeezing parameters $r > 0.20$ for Fig. 2a, $r > 0.28$ for Fig. 2b, and $r > 0.35$ for Fig. 2c, the correlation variances (curve 1) are smaller than the boundary for the case of $g = 1$. It means that if taking $g = 1$, a lower limitation for the squeezing parameter is required to satisfy each of the inseparability criteria. However, if taking the optimal gain factor g^{opt} (curve 3) all variances are below the boundary for any values of $r > 0$.

III. EXPERIMENTAL DETAILS

The four NOPAs were constructed in identical configuration, each of which consists of an α -cut type-II KTP crystal and a concave mirror [5]. The front face of the KTP was coated to be used for the input coupler and the concave mirror serves as the output coupler of the squeezed states, which was mounted on a piezo-electric transducer for locking actively the cavity length of NOPA on resonance with the injected signal at 1080 nm. The transmissions of the input coupler for the pump laser at 540 nm and the injected signal at 1080 nm are 99.8% and 0.04%, respectively. The transmissions of the output coupler at 540 nm and 1080 nm are 0.5% and 5.2%, respectively. The finesses of the NOPA for 540 nm and 1080 nm are 3 and 117, respectively. Through the intracavity parametric down conversion

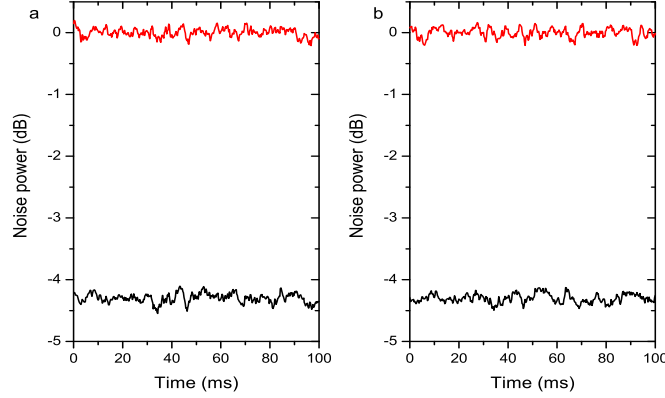


FIG. 7: The measured noise power of initial squeezed state. a and b are amplitude and phase quadrature, respectively. Red and black lines are the noise power for the QNL and the squeezed state, respectively.

process of type-II phase match, the two quadrature squeezed states of light at 1080 nm were produced [6, 7]. The squeezing parameter r depends on the strength and the time of parametric interaction in the NOPA. In the calculations we have assumed that squeezing parameter for the eight squeezed states is identical for simplicity and without losing the generality. The requirement is easy to be reached in the experiments if the four NOPAs were constructed in identical configuration and the intracavity losses of the signal and the idler modes in each NOPA were balanced. The experimentally measured squeezing degrees of the output fields from four NOPAs are about 4.30 ± 0.07 dB below the corresponding QNL, which are shown in Fig. 3, a and b stand for quadrature-amplitude and quadrature-phase squeezing, respectively.

Four NOPAs are locked individually by using Pound-Drever-Hall (PDH) method with a phase modulation of 56 MHz on 1080 nm laser beam [8]. Each NOPA is operated at deamplification condition, which corresponds to lock the relative phase between the pump laser and the injected signal to $(2n+1)\pi$ (n is the integer). In the experiment, the relative phase locking is completed with a lock-in amplifier, where a signal at 15 kHz is modulated on the pump light by the piezo-electric transducer (PZT) mounted on a reflection mirror which is placed in the optical path of the pump laser and then the error signal is fed back to the other PZT which is mounted on a mirror placed in the optical path of the injected beam.

In the beam-splitter network used to prepare eight-partite cluster states, T1 is phase-locked to zero, T2-T7 is phase-locked to $\pi/2$. The zero phase difference (T1) between two interfered beams on a beam-splitter is locked by a lock-in amplifier with a modulation of 12 kHz. The $\pi/2$ phase difference (T2-T7) is locked by DC locking technique, where the photocurrent signal of the interference fringe is fed back to the PZT mounted on a mirror which is placed before the beam-splitter.

In the homodyne detection system, zero phase difference for the measurement of quadrature-amplitude is locked by PDH technique with a phase modulation of 10.9 MHz on local oscillator beam. The $\pi/2$ phase for the measurement of quadrature-phase is locked by using DC locking technique too.

-
- [1] P. van Loock, C. Woodbrook, and Mile Gu, Phys. Rev. A **76**, 032321 (2007).
 - [2] J. Zhang and S. L. Braunstein, Phys. Rev. A **73**, 032318 (2006).
 - [3] Nicolas C. Menicucci, Steven T. Flammia, and Peter van Loock, Phys. Rev. A **83**, 042335 (2011).
 - [4] P. van Loock, and A. Furusawa, Phys. Rev. A **67**, 052315 (2003).
 - [5] Y. Wang, H. Shen, X. Jin, X. L. Su, C. D. Xie, and K. C. Peng, Opt. Express, **18**, 6149-6155 (2010).
 - [6] M. D. Reid, Phys. Rev. A **40**, 913 (1989).
 - [7] Y. Zhang, Hai Wang, Xiaoying Li, Jietai Jing, Changde Xie, and Kunchi Peng, Phys. Rev. A **62**, 023813 (2000).
 - [8] R. W. P. Drever, J. L. Hall, F. V. Kowalski J. Hough, G. M. Ford, A. J. Munley, and H. Ward, Appl. Phys. B: Photophys. Laser Chem. **31**, 97-105 (1983).